

## Supporting Information

### Thermodynamic Study of Crown Ether–Lithium/Magnesium Complexes based on Benz-1,4-Dioxane and its Homologues

Iklima Oral,<sup>a</sup> Fanny Ott,<sup>a</sup> and Volker Abetz<sup>a,b,\*</sup>

<sup>a</sup> Institute of Physical Chemistry, Universität Hamburg, Grindelallee 117, 20146 Hamburg, Germany.

<sup>b</sup> Helmholtz-Zentrum Hereon, Institute of Membrane Research, Max-Planck-Straße 1, 21502 Geesthacht, Germany. E-mail: volker.abetz@hereon.de

## Benzo-7-crown-2

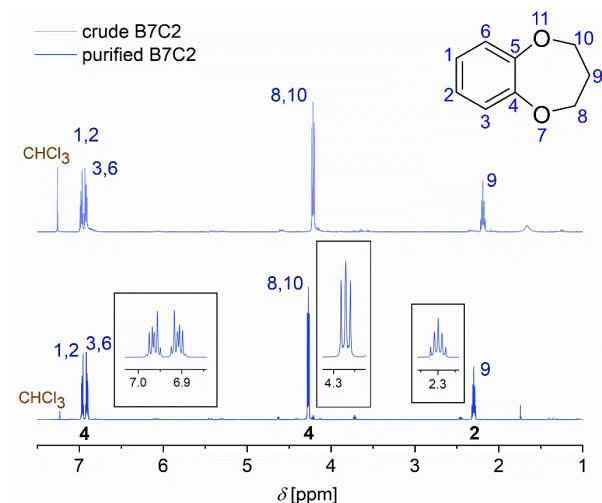


**Fig. S1:** <sup>1</sup>H NMR spectrum of the crude B7C2 and purified B7C2 after column chromatography treatment.

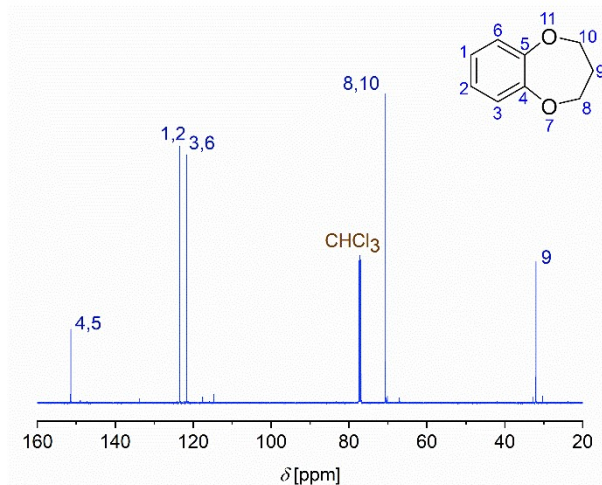


**Fig. S2:** <sup>13</sup>C NMR spectrum of the purified B7C2.

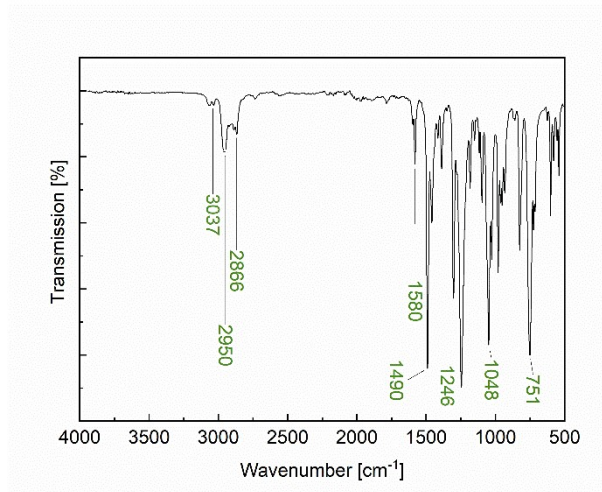


**Fig. S3:** IR spectrum of the purified B7C2.

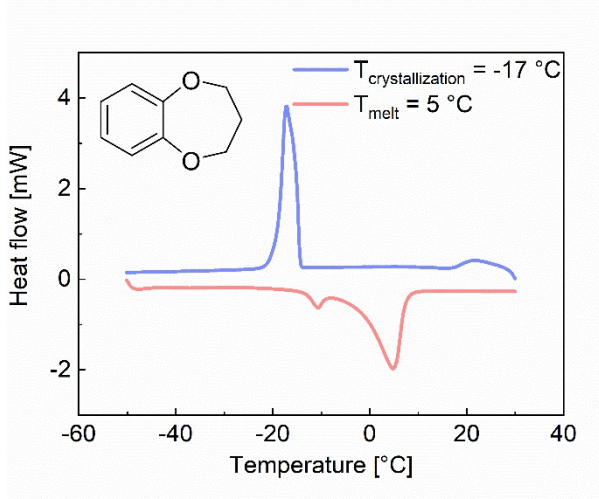


**Fig. S4:** DSC measurement of the purified B7C2.

### Benzo-8-crown-2

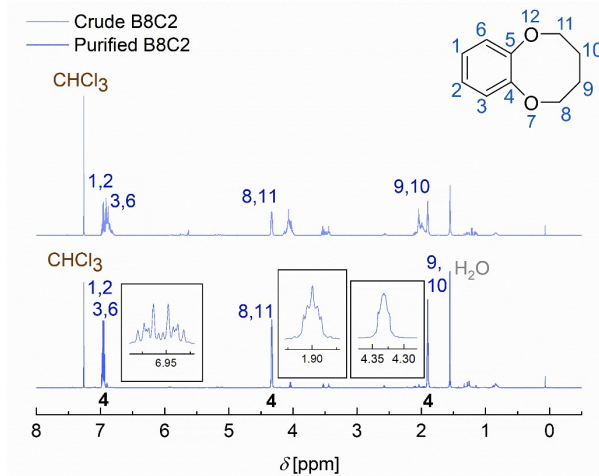


**Fig. S5:**  ${}^1\text{H}$  NMR spectrum of the crude B8C2 and purified B7C2 after column chromatography treatment.

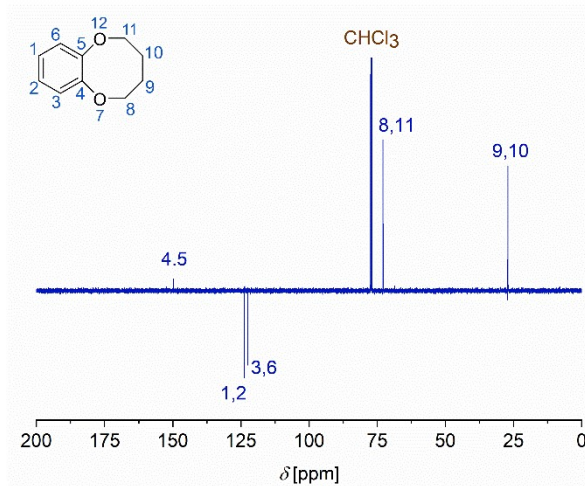


**Fig. S6:**  ${}^{13}\text{C}$  NMR spectrum of the purified B8C2.

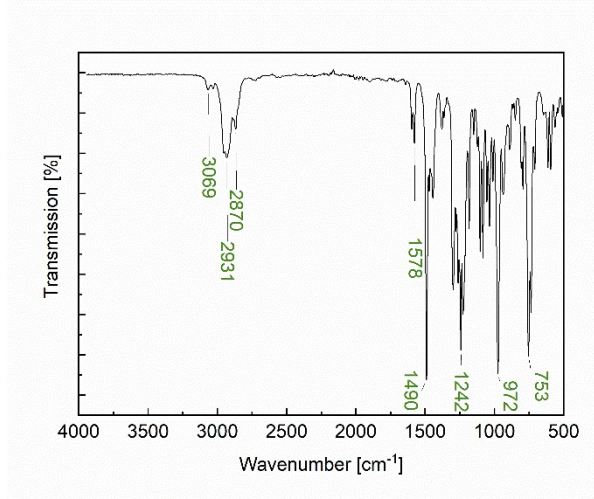


**Fig. S7:** IR spectrum of the purified B8C2.

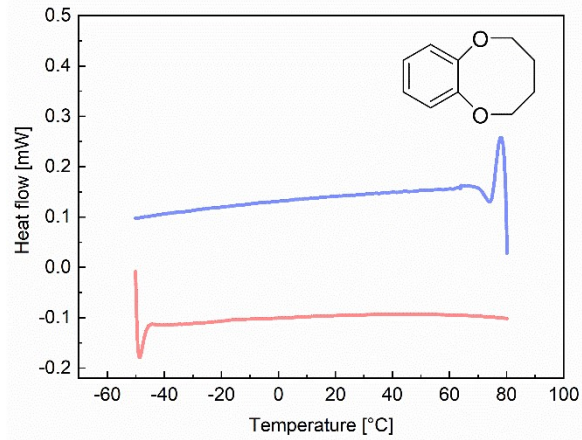


**Fig. S8:** DSC measurement of the purified B8C2.

### UV-vis Data

#### Lithium

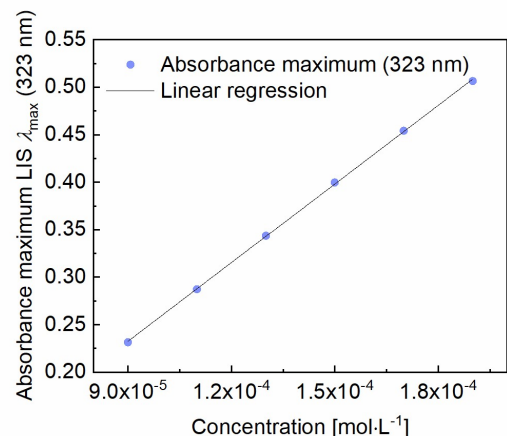


**Fig. S9:** Absorbance maxima of LIS  $\lambda_{\max} = 323 \text{ nm}$  as linear regression against concentration [ $\text{mol} \cdot \text{L}^{-1}$ ].

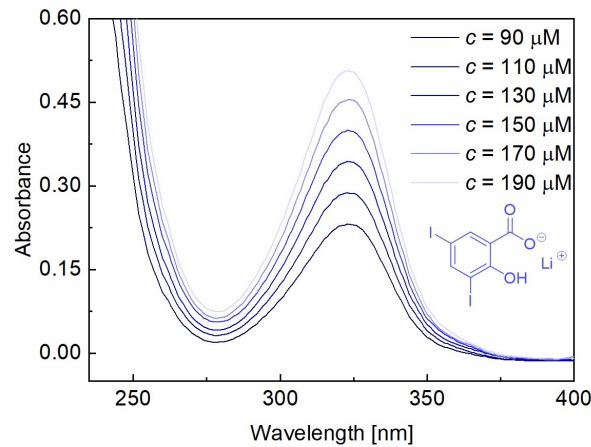


**Fig. S10:** UV-vis spectrum of LIS at different concentrations [ $\mu\text{mol}\cdot\text{L}^{-1}$ ].

## Magnesium

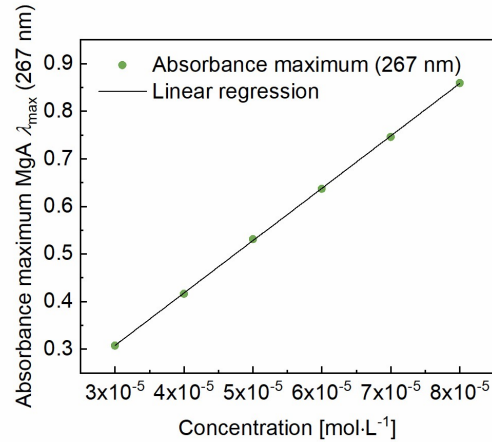


**Fig. S11:** Absorbance maxima of MgA  $\lambda_{\max} = 267 \text{ nm}$  as linear regression against concentration [ $\text{mol}\cdot\text{L}^{-1}$ ].

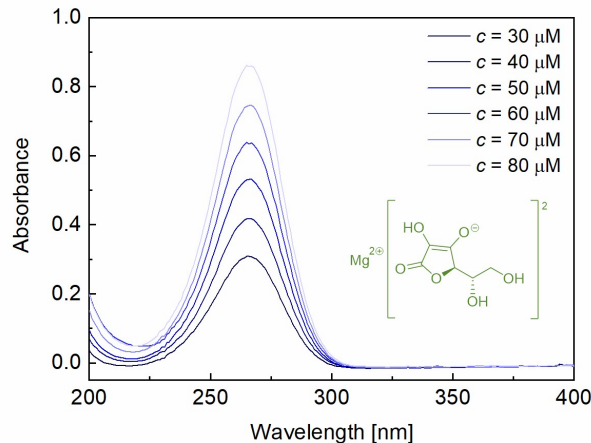


**Fig. S12:** UV-vis spectrum of MgA at different concentrations [ $\mu\text{mol}\cdot\text{L}^{-1}$ ].

### CE solubility measurements in the aqueous phase

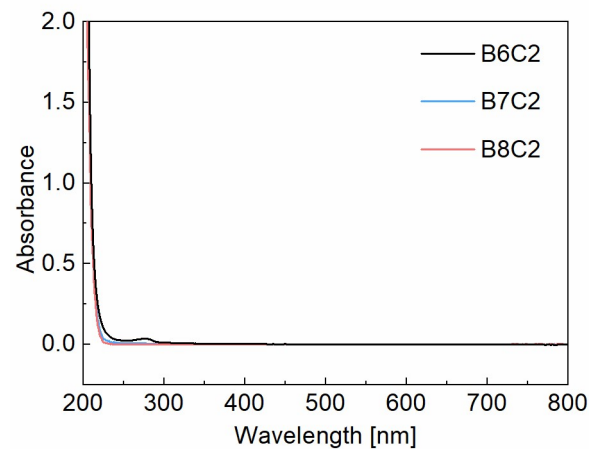


**Fig. S13:** UV-vis spectroscopy of the aqueous LiCl phase after extraction and formation of the CE–cation complex.

## Thermodynamic Evaluation

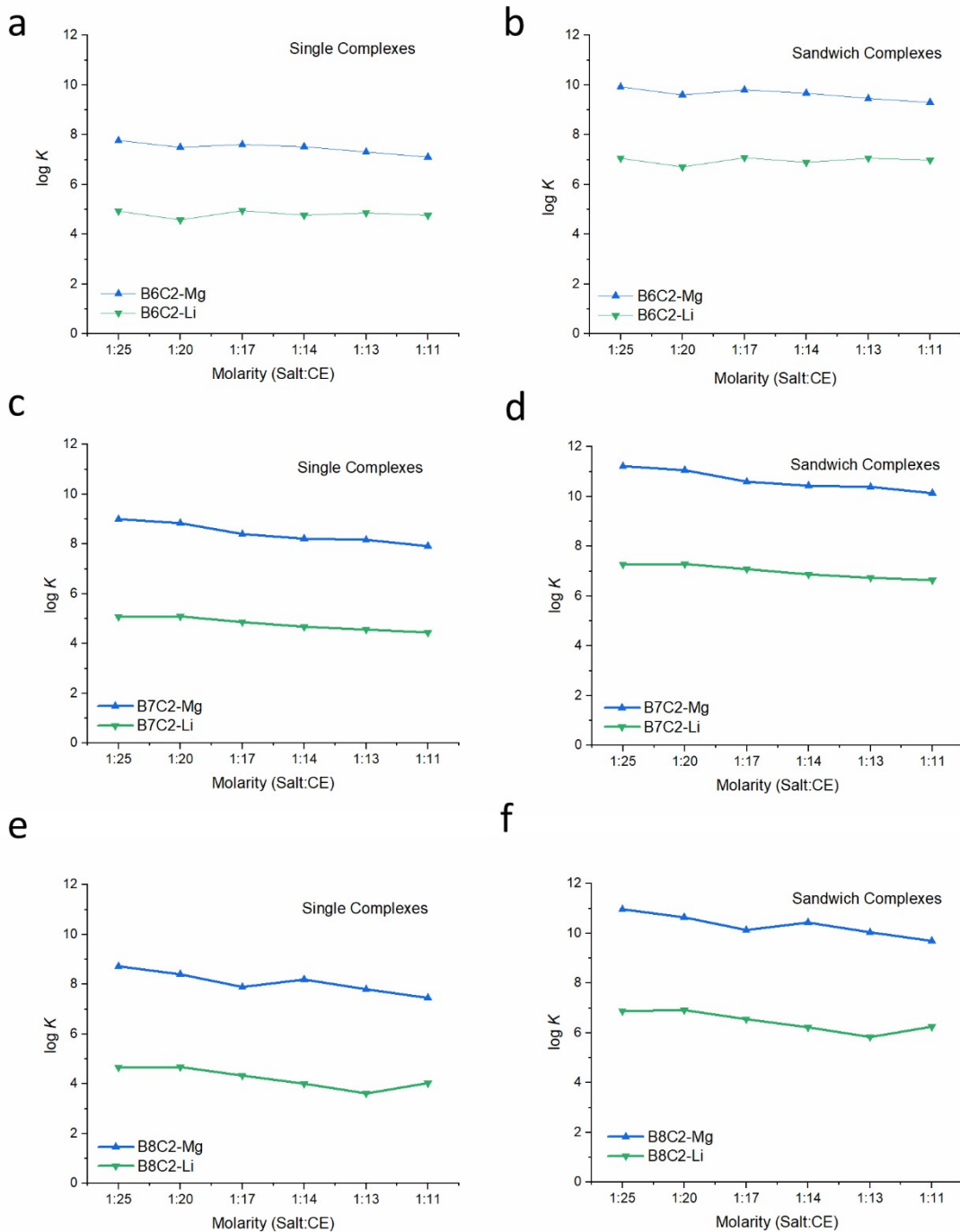


**Fig. S14:** logarithmic complexation stability  $K$  of a) B6C2 assuming single complexes, b) B6C2 assuming sandwich-type complexes, c) B7C2 assuming single complexes, d) B7C2 assuming sandwich-type complexes, e) B8C2 assuming single complexes, f) B8C2 assuming sandwich-type complexes. The green line shows the lithium, and the blue line the magnesium complexes with the CEs.

## Van't Hoff Plot

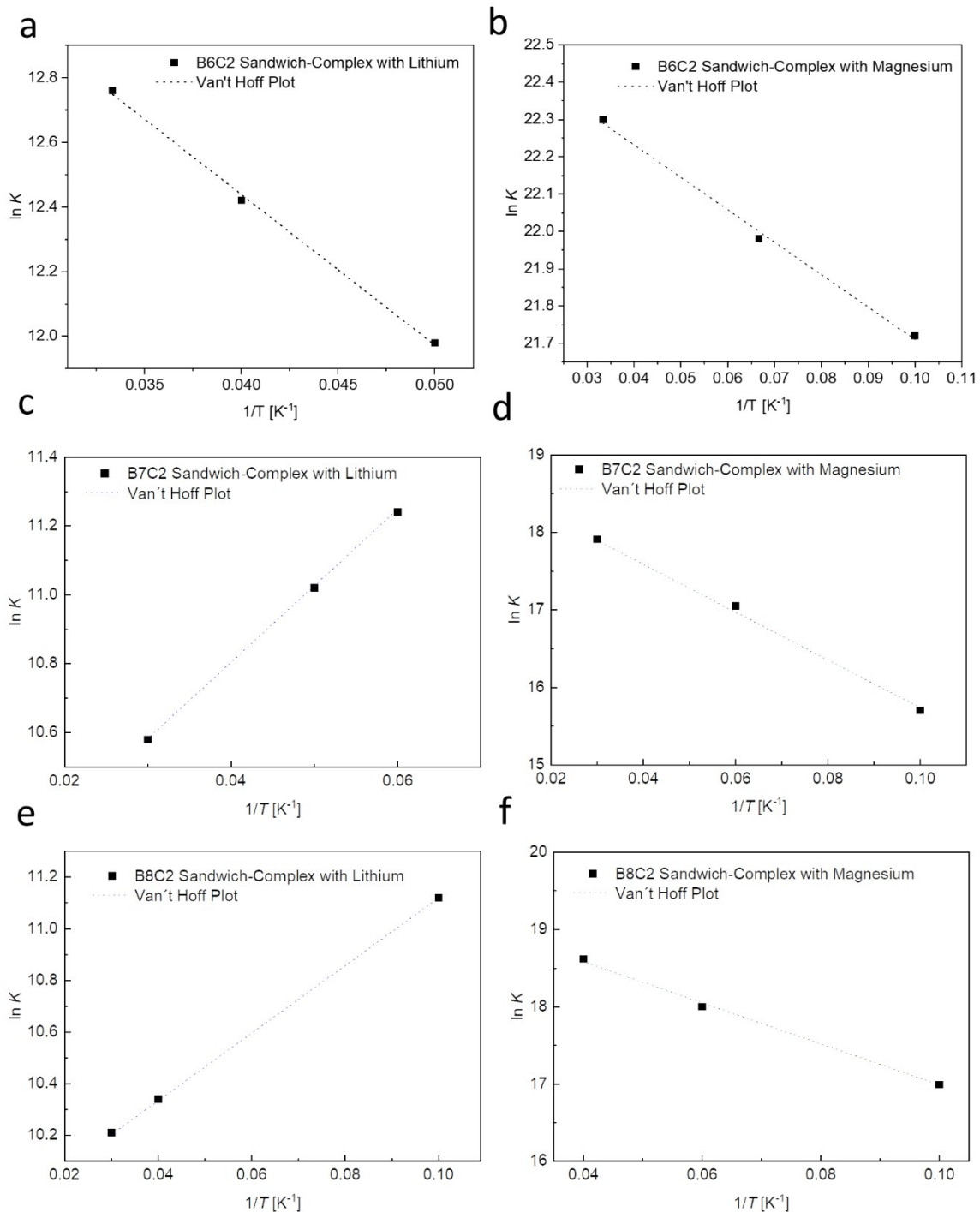


**Fig. S15:** Van't Hoff plot of the a) B6C2-Li complex b) B6C2-Mg complex, c) B7C2-Li complex, d) B7C2-Mg complex, e) B8C2-Li complex, and f) B8C2-Mg complex with a constant molar ratio of CE:salt = 14:1.

**Tab. S1:** Log  $K$  and Gibbs energy  $\Delta G$  at 25 °C of the extraction of B6C2, B7C2 and B8C2 with Li<sup>+</sup> and Mg<sup>2+</sup>.

<b>B6C2-Li<sup>+</sup></b>	<b>Single</b>		<b>Sandwich</b>	
CE:metal	log $K$	$\Delta G$ [kJmol <sup>-1</sup> ]	log $K$	$\Delta G$ [kJmol <sup>-1</sup> ]
1:25	4.9	-28	7.06	-40
1:20	4.6	-26	6.71	-38
1:17	5.0	-28	7.07	-40
1:14	4.8	-27	6.89	-40
1:13	4.9	-28	7.05	-40
1:11	4.8	-27	6.98	-40
<b>B6C2-Mg<sup>2+</sup></b>	<b>Single</b>		<b>Sandwich</b>	
CE:metal	log $K$	$\Delta G$ [kJmol <sup>-1</sup> ]	log $K$	$\Delta G$ [kJmol <sup>-1</sup> ]
1:25	7.8	-44	9.9	-57
1:20	7.5	-43	9.6	-55
1:17	7.6	-44	9.8	-56
1:14	7.5	-43	9.7	-55
1:13	7.3	-42	9.5	-54
1:11	7.1	-41	9.3	-53
<b>B7C2-Li<sup>+</sup></b>	<b>Single</b>		<b>Sandwich</b>	
CE:metal	log $K$	$\Delta G$ [kJmol <sup>-1</sup> ]	log $K$	$\Delta G$ [kJmol <sup>-1</sup> ]
1:25	5.1	-29	7.3	-42
1:20	5.1	-29	7.3	-42
1:17	4.9	-28	7.1	-40
1:14	4.7	-27	6.9	-39
1:13	4.6	-25	6.7	-39
1:11	4.5	-25	6.7	-38
<b>B7C2-Mg<sup>2+</sup></b>	<b>Single</b>		<b>Sandwich</b>	
CE:metal	log $K$	$\Delta G$ [kJmol <sup>-1</sup> ]	log $K$	$\Delta G$ [kJmol <sup>-1</sup> ]
1:25	9.0	-51	11	-64
1:20	8.8	-50	11	-63
1:17	8.4	-48	11	-61
1:14	8.2	-47	10	-60
1:13	7.9	-45	10	-59
1:11	7.6	-43	10	-58
<b>B8C2-Li<sup>+</sup></b>	<b>Single</b>		<b>Sandwich</b>	
CE:metal	log $K$	$\Delta G$ [kJmol <sup>-1</sup> ]	log $K$	$\Delta G$ [kJmol <sup>-1</sup> ]
1:25	4.7	-27	6.9	-39
1:20	4.7	-27	6.9	-39
1:17	4.3	-25	6.6	-37
1:14	4.0	-23	6.2	-36
1:13	3.6	-21	5.8	-33
1:11	4.0	-20	6.3	-36
<b>B8C2-Mg<sup>2+</sup></b>	<b>Single</b>		<b>Sandwich</b>	
CE:metal	log $K$	$\Delta G$ [kJmol <sup>-1</sup> ]	log $K$	$\Delta G$ [kJmol <sup>-1</sup> ]
1:25	8.7	-50	11	-63
1:20	8.4	-48	11	-61
1:17	7.9	-45	10	-58
1:14	8.2	-47	10	-60
1:13	7.8	-45	10	-57
1:11	7.5	-43	9.1	-55

**Tab. S2:** Slope and intercept values of the Van't Hoff plot and the determined data of  $\Delta H$ ,  $\Delta S$  and  $\Delta G$  (at 25 °C).

$\text{Li}^+$	$R^2$	Slope $\left( \frac{-\Delta H}{R} \right)$	Intercept $\left( \frac{\Delta S}{R} \right)$	$\Delta H [\text{Jmol}^{-1}]$	$\Delta S [\text{Jmol}^{-1}\text{K}^{-1}]$	$\Delta G \text{ VH } [\text{kJmol}^{-1}]$
<b>B6C2</b>	0.997	-46.6	14.3	387	119	-35
<b>B7C2</b>	0.998	20.1	15.0	-167	125	-37
<b>B8C2</b>	0.999	13.7	14.9	-114	124	-37
$\text{Mg}^{2+}$	$R^2$	Slope $\left( \frac{-\Delta H}{R} \right)$	Intercept $\left( \frac{\Delta S}{R} \right)$	$\Delta H [\text{Jmol}^{-1}]$	$\Delta S [\text{Jmol}^{-1}\text{K}^{-1}]$	$\Delta G \text{ VH } [\text{kJmol}^{-1}]$
<b>B6C2</b>	0.993	-8.70	22.6	72.3	188	-56
<b>B7C2</b>	0.997	-31.7	23.9	263	199	-59
<b>B8C2</b>	0.995	-28.0	25.0	233	208	-62